Laser Photoelectron Spectroscopy and Dynamics of S_1 *p*-Fluorotoluene

Susan M. Bellm, Paul T. Whiteside, and Katharine L. Reid*

School of Chemistry, University of Nottingham, Nottingham NG7 2RD, United Kingdom

Received: March 18, 2003; In Final Form: June 16, 2003

Laser photoelectron spectra have been obtained following the preparation of 10 vibrational states in S_1 *p*-fluorotoluene. For eight of the vibrational states (up to ∼850 cm^{-1} excess energy), excitation and ionization with nanosecond laser pulses gives rise to photoelectron spectra with well-resolved vibrational peaks. For the other two states (>1100 cm^{-1} excess energy), the photoelectron spectra show a loss of structure when nanosecond pulses are used, as a result of intramolecular dynamics, but this structure is recovered when overlapped picosecond pulses are used. In all cases the vibrational peaks in the photoelectron spectra are assigned, and the spectra are used to deduce the frequencies of 12 vibrational modes in the ion.

Introduction

Laser photoelectron spectroscopy (PES) is well-suited to the study of small aromatic molecules whose S_1 electronic states and ionization potentials typically lie at around 4.5 and 9 eV, respectively, enabling one-color (1 + 1) resonance-enhanced multiphoton ionization (REMPI) experiments to be performed. Such REMPI-PES experiments, which have the advantage of state selection prior to ionization, provide information both on S_1 spectroscopy and dynamics and, through the photoelectron spectra of different S_1 vibrational modes, on the spectroscopy of the ion ground state. A number of such molecules have been studied by this means, including benzene,[1] *p*-difluorobenzene,[2] toluene,[3] and phenol.[4]

Our interest in *p*-fluorotoluene (pFT) was stimulated by the intramolecular vibrational energy redistribution (IVR) dynamics it exhibits in its S_1 excited electronic state. In this electronic state pFT appears to show anomalous IVR lifetimes when compared with the very similar molecule *p*-difluorobenzene (pDFB). Moss and Parmenter[5] have reported that whereas S_1 pDFB with an excitation energy of ∼2000 cm^{-1} has an estimated IVR lifetime of 150 ps, S_1 pFT with the same excitation energy has an estimated IVR lifetime of 3.5 ps. In the course of our own investigations of these dynamics by picosecond pump−probe photoelectron spectroscopy,[6] it became apparent that although S_1 pFT has been extensively studied by laser excitation and fluorescence[7,8] the photoelectron spectroscopy following ionization from S_1 and the vibrational frequencies of its ion ground state were unknown. Although there is a ZEKE study of pFT in the literature,[9] this concentrates on the torsional motion of the methyl rotor and other vibrational modes were not probed.

In this paper we present a comprehensive and systematic investigation of the photoelectron spectroscopy of pFT that has been prepared in a series of S_1 vibrational states prior to ionization, covering S_1 excitation energies up to 1230 cm^{-1}. We present photoelectron spectra taken with both nanosecond and picosecond laser pulses and show that whereas vibrational resolution is achieved in the nanosecond case for excitation energies up to 845 cm^{-1}, this resolution is lost for S_1 excitation energies greater than ∼1100 cm^{-1} as a consequence of IVR. The vibrational resolution is recoverable at these higher excitation energies when picosecond laser pulses are used. From the assignments we have made of the photoelectron spectra we have been able to deduce approximate vibrational frequencies for 12 vibrational modes in the electronic ground state of the ion.

Experimental Section

The apparatus has been described in detail in previous publications from this group;[10] here we provide a brief description and report details relevant to this work.

Room temperature *p*-fluorotoluene (Aldrich, 99%) was seeded in helium and expanded through a pulsed nozzle (General Valve) into a skimmed molecular beam chamber. The skimmed molecular beam was intersected perpendicularly by a loosely focused laser beam at one end of a 24 cm long, doubly μ-metal shielded drift tube. All surfaces on the inside of the drift tube were coated with graphite to minimize the buildup of contact potentials and so providing an almost completely field-free environment.

Two independent laser sources were used to generate UV light resonant with $S_1 \leftarrow S_0$ vibronic transitions of pFT. Light pulses of approximately 5 ns duration were produced by using a 10 Hz Nd:YAG laser (Continuum Surelite III) to pump a dye laser (Continuum ND6000) operating with either LDS 750 or LDS 698 dye. The dye laser system was equipped with an UVT autotracking unit in which the dye beam was first doubled in a KDP crystal and then mixed with the fundamental from the Nd:YAG laser in a second KDP crystal to generate light in the range 260−272 nm.

Light pulses of approximately 1 ps duration were produced with a titanium sapphire regenerative amplifier (RGA, Spectra-Physics Spitfire) configured for the chirped pulse amplification of picosecond pulses. The RGA was seeded by a self-mode locked titanium sapphire laser (Spectra-Physics Tsunami). The output pulses from the RGA were used to pump an optical parametric amplifier (OPA) providing tunable light in the region of 260 nm with a bandwidth of around 20 cm^{-1}. Experiments involving these picosecond pulses were carried out in the Lasers for Science Facility at the Rutherford-Appleton Laboratory.

Photoelectrons formed by one-color (1 + 1) REMPI and ejected along the axis of the drift tube were detected with a 2.5 cm diameter triple microchannel plate detector (Photek) mounted at the other end, thus giving a small solid angle of detection. The photoelectron signal was passed through an amplifier (Ortec

10.1021/jp030341+ CCC: $25.00

TABLE 1: Vibrational Modes and Frequencies of *p*-Fluorotoluene and *p*-Difluorobenzene in Their S_0 and S_1 Electronic States and Ground Ion State[a]

	p-fluorotoluene						*p*-difluorobenzene			
	C_{2v}	S_0[b] (cm^{-1})	S_1[b] (cm^{-1})	D_0[c] (cm^{-1})	descriptions[d]		D_{2h}	S_0[e] (cm^{-1})	S_1[e] (cm^{-1})	D_0[e] (cm^{-1})
1	A_1	3071			CH stretch	1	A_g	3088		
2	A_1	3068			CH stretch	10	B_{1u}	3089		
3	A_1	2925			CH stretch					
4	A_1	1607		1575 ± 20	ring stretch	2	A_g	1617		1640
5	A_1	1509			CH rock	11	B_{1u}	1508	1339	
6	A_1	1380			CH_3 umbrella					
7	A_1	1223	1230	1344 ± 20	CF stretch	3	A_g	1257	1251	1375
8	A_1	1214	1194	1200 ± 20	CH_3−C stretch	12	B_{1u}	1210	1016	
9	A_1	1155		1122 ± 20	CH rock	4	A_g	1140	1116	1148
10	A_1	1017	845	944 ± 20	ring bend	13	B_{1u}	1016	936	
11	A_1	844	803	786 ± 20	ring breathing	5	A_g	860	818	836
12	A_1	728			CH_3−C stretch	14	B_{1u}	734		
13	A_1	455	408	418 ± 20	ring breathing	6	A_g	450	410	439
14	A_2	956			CH out of plane	7	A_u	945	583	
15	A_2	810			CH out of plane	9	B_{1g}	798		
16	A_2	404	199	328 ± 20	ring twist	8	A_u	422	179	359
17	B_1	2952			CH stretch					
18	B_1	1455			CH_2 scissors					
19	B_1	1041			CH_2 rock					
20	B_1	927			CH out of plane	15	B_{2g}	927		
21	B_1	638			CH out of plane	28	B_{3u}	831		
22	B_1	816			chair def	16	B_{2g}	694		
23	B_1	492	435		CF out of plane	29	B_{3u}	508	436	508
24	B_1	340	255		CH_3 wag	17	B_{2g}	379	274	
25	B_1	157	137	150 ± 20	boat def	30	B_{3u}	161	122	129
26	B_2	3089[f]			CH stretch	23	B_{3g}	3081		
27	B_2	3040			CH stretch	18	B_{2u}	3089		
28	B_2	2976			CH stretch					
29	B_2	1592			ring stretch	24	B_{3g}	1621		
30	B_2	1463[f]			CH_3 def					
31	B_2	1435			ring stretch	19	B_{2u}	1436		
32	B_2	1321			CH rock	20	B_{2u}	1282	1589	
33	B_2	1300			ring stretch	25	B_{3g}	1282		
34	B_2	1099			CH rock	21	B_{2u}	1089	1097	
35	B_2	988[f]			CH_2 rock					
36	B_2	638	549	578 ± 20	ring bend	26	B_{3g}	635		
37	B_2	420	399	383 ± 20	CF rock	27	B_{3g}	436	395	
38	B_2	312	219	222 ± 20	CH_3 rock	22	B_{2u}	347	355	

[a] Vibrational modes are numbered by the Mulliken notation.[12] In the case of pFT, the assigned symmetries neglect the methyl group. [b] Taken from ref 7. [c] This work. [d] Taken from ref 11. [e] Taken from ref 2. [f] Calculated frequencies (ref 11).

×10) and the flight times of the photoelectrons were recorded with a time-to-digital converter (TDC, LeCroy 2277), which has a time resolution of 1 ns. The TDC was controlled and read by a PC via a CAMAC interface (Hytec Electronics). Photoelectron spectra caused by the ejection of photoelectrons along the direction of the polarization vector of the ionizing light were accumulated over approximately 100 000 laser shots. Although some sample photoelectron angular distributions were also measured by rotating the polarization vector of the ionizing light, there was no evidence of any significant change in the branching ratios of the ion states formed with ejection angle and so the photoelectron spectra taken at one angle are representative of the angle-integrated photoelectron spectra.

Results

Photoelectron time-of-flight spectra were obtained for jet-cooled pFT as described in the previous section with the nanosecond dye laser resonant with 10 $S_1 \leftarrow S_0$ vibronic transitions (excess energy in S_1 is given in parentheses): 0^0_0, 25^1_0 (137 cm^{-1}), 38^1_0 (219 cm^{-1}), the unresolved pair $37^1_0 + 16^2_0$ (399 cm^{-1}), 13^1_0(408 cm^{-1}), 36^1_0 (549 cm^{-1}), 11^1_0 (803 cm^{-1}), 10^1_0 (845 cm^{-1}), 8^1_0 (1194 cm^{-1}), and 7^1_0 (1230 cm^{-1}). The excess energy available to the ion ground state (D_0) following (1 + 1) REMPI varies from ~2000 cm^{-1} (0^0_0) to ~5000 cm^{-1} (7^1_0). The nature of the vibrational modes is given in Table 1, following ref 11; those excited represent the main active modes following one-photon excitation from S_0.[7,8] There are various conventions used to number the vibrational modes in the literature;[7,8] we have used strict Mulliken notation.[12] The excited modes ν_{25}, ν_{36}, ν_{37}, and ν_{38} are nontotally symmetric; the activity of these modes is believed to result from vibronic coupling, in analogy with behavior in pDFB.[13]

The flight times were converted to ion internal energy by use of the known pFT ionization potential[9] of 70 940 cm^{-1} in order that assignments could be made. This conversion process required the application of a correction to both the flight times (Δt) and the photoelectron energy (ΔE) to allow for the imperfect conditions in the flight tube, as is usual in time-of-flight photoelectron spectroscopy.[1−4] To establish appropriate values for these two parameters, peaks believed to be due to the vibrationless level in the ion were corrected to appear at zero ion energy in such a fashion that the same two parameters could be used for all photoelectron spectra. The resulting, rather large, values for the two parameters were $\Delta t = +40$ ns and $\Delta E = -320$ cm^{-1}. Despite these large corrections we have confidence in our assignments owing to the self-consistency of the resulting 10 photoelectron spectra, their analogy with the corresponding photoelectron spectra for pDFB, which has

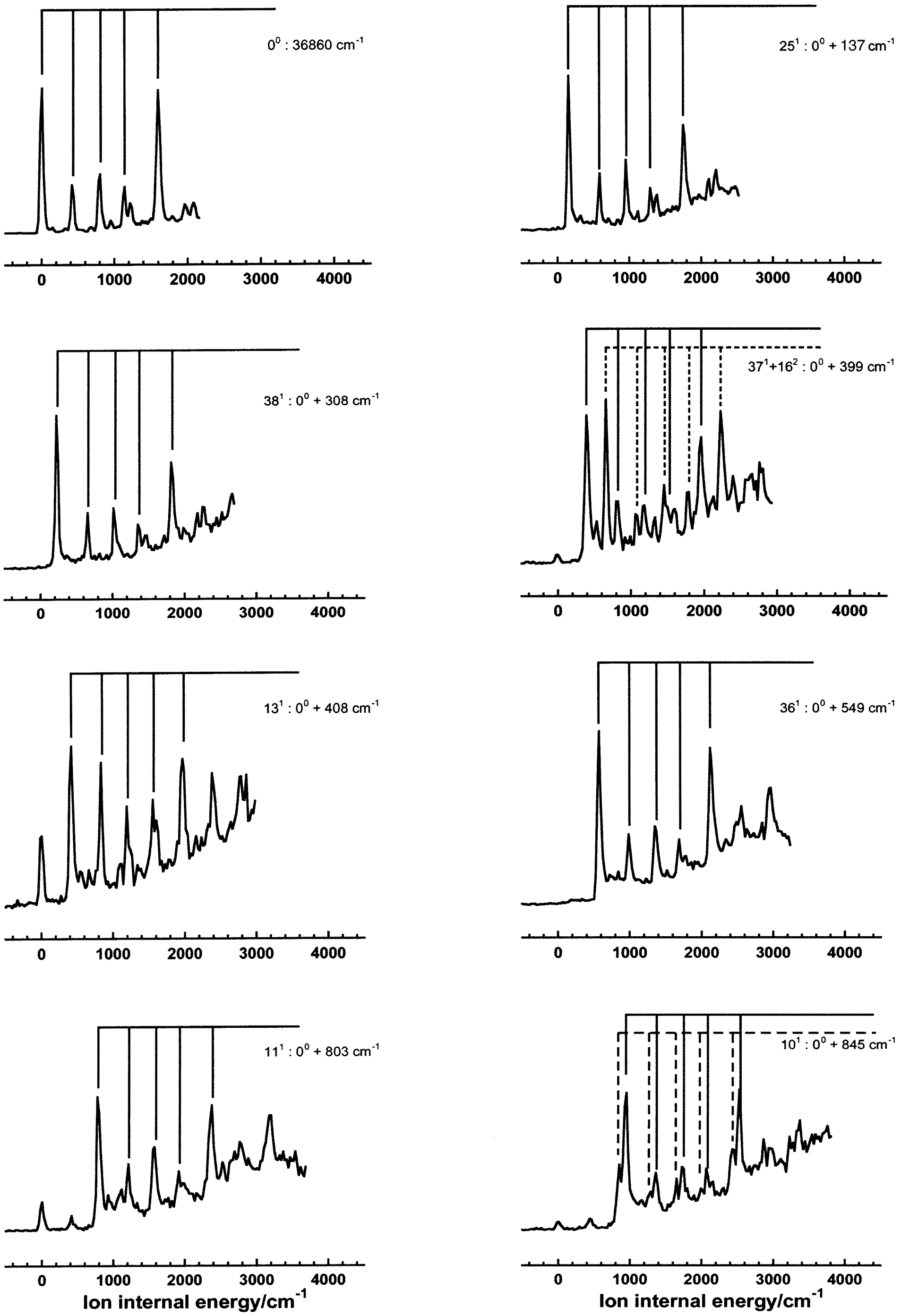

Figure 1. Nanosecond photoelectron spectra following the excitation of eight $S_1 \leftarrow S_0$ bands as labeled on each spectrum, and ionization with the same wavelength. On each spectrum the characteristic series X^m, X^m13^1, X^m11^1, X^m9^1, and X^m4^1, where *m* quanta of mode X have been prepared in S_1, has been labeled.

similar excitation spectra[2,14] (see later), and the values of the ion vibrational frequencies obtained that compare sensibly with the values of the vibrational frequencies both in neutral pFT[7,8] and in the pDFB ion.[2,14]

Because the pFT ion vibrational frequencies were unknown, our assignments of peaks in the photoelectron spectra made use of the fact that only small changes are expected from the frequencies of the same modes in the neutral parent ground and first excited states,[15] which are known from laser-induced fluorescence and dispersed fluorescence spectra.[7,8] The resulting converted and assigned photoelectron spectra for the eight lowest energy modes are shown in Figure 1, and the energies and assignments of the peaks, which all have fwhm values of 50−70 cm^{-1}, are shown in Table 2. It will be seen that the peak energies deduced are consistent from spectrum to spectrum to within ±20 cm^{-1} and that the spectra all show vibrationally resolved peaks. Ion vibrational frequencies, deduced by taking averages of the values determined from the photoelectron spectra, have been included in Table 1 for comparison with the frequencies in the S_0 and S_1 electronic states of the neutral molecule.

Two relevant studies of the related molecule pDFB exist in the literature with which we can make comparisons; Table 1 includes complementary vibrational frequencies and mode labels for this molecule. The first study describes REMPI-PES experiments performed by Reilly and co-workers[2] in which 10

TABLE 2: Peak Positions and Assignments of the Ten Vibrationally Resolved Spectra[a]

assignments	0_0^0	25_0^1	38_0^1	$37_0^1 + 16_0^2$	13_0^1	36_0^1	11_0^1	10_0^1	8_0^1	7_0^1
0^0	0			0	0		0	0	0	
25^1	150	150								
38^1			222							
16^1	328									
37^1				383						
13^1	417				411		417	433	411	
36^1						578				
$13^1 25^1$		583			556					
16^2				656						
$13^1 38^1$			656							
$25^1 36^1$						729				
11^1	789						783			
$13^1 37^1$				811						
13^2					822					
10^1	944							944		
$11^1 25^1$		950					933			
$13^1 36^1$						989				
$11^1 38^1$			1022							
$13^1 16^2$				1072						
9^1	1133				1111					
$11^1 16^1$							1117			
$11^1 37^1$				1172						
8^1									1200	
$11^1 13^1$	1211				1183		1211			
$9^1 25^1$		1289								
7^1										1344
$11^1 36^1$						1350				
$9^1 38^1$			1356							
$10^1 13^1$								1361		
$11^1 13^1 25^1$		1389								
$11^1 16^2$				1450						
$11^1 13^1 38^1$			1466							
$9^1 37^1$				1483						
$9^1 13^1$					1533					
4^1 $(+11^2)$	1583						1567			
$11^1 13^1 37^1$				1589						
$11^1 13^2$					1600					
$8^1 13^1$									1622	
$9^1 36^1$						1689				
$10^1 11^1$								1733		
$4^1 25^1$ $(+11^2 25^1)$		1750								
$7^1 13^1$										1755
$11^1 13^1 36^1$						1772				
$9^1 16^2$				1778						
$4^1 38^1$ $(+11^2 38^1)$			1822							
$11^1 13^1 16^2$				1867						
$9^1 11^1$	1967						1911			
$4^1 37^1$ $(+11^2 37^1)$				1956						
$4^1 13^1$ $(+11^2 13^1)$	2083				1956		1983			
$8^1 11^1$									2017	
$9^1 10^1$								2067		
$9^1 11^1 25^1$		2106								
$7^1 11^1$										2117
$4^1 36^1$ $(+11^2 36^1)$						2133				
$10^1 11^1 13^1$								2156		
$9^1 11^1 38^1$			2178							
$4^1 13^1 25^1$ $(+11^2 13^1 25^1)$		2206								
$4^1 16^2$ $(+11^2 16^2)$				2228						
$4^1 13^1 38^1$ $(+11^2 13^1 38^1)$			2256							
$9^1 11^1 13^1$					2328					
$8^1 9^1$									2356	
$4^1 11^1$ $(+11^3)$							2367			
$4^1 13^2$ $(+11^2 13^2)$					2378					
$8^1 11^1 13^1$									2433	
$7^1 9^1$										2456
$9^1 11^1 36^1$						2489				
$4^1 10^1$ $(+10^1 11^2)$								2528		
$7^1 11^1 13^1$										2528
$4^1 13^1 36^1$ $(+11^2 13^1 36^1)$						2561				
$4^1 11^1 38^1$ $(+11^3 38^1)$			2661							
$4^1 9^1$ $(+9^1 11^2)$							2700			
$4^1 11^1 13^1$ $(+11^3 13^1)$					2756		2772			
$4^1 8^1$ $(+8^1 11^2)$									2811	

TABLE 2 (Continued)

assignments	0_0^0	25_0^1	38_0^1	$37_0^1 + 16_0^2$	13_0^1	36_0^1	11_0^1	10_0^1	8_0^1	7_0^1
$4^1 7^1$ $(+7^1 11^2)$										2894
$4^1 11^1 36^1$ $(+11^3 36^1)$						2939				
$4^1 10^1 13^1$ $(+10^1 11^2 13^1)$								2956		
4^2 $(+11^4)$							3178			
$4^1 8^1 13^1$ $(+8^1 11^2 13^1)$									3222	
$4^1 7^1 13^1$ $(+7^1 11^2 13^1)$										3294
$4^1 10^1 11^1$ $(+10^1 11^3)$								3344		
$4^1 9^1 11^1$ $(+9^1 11^3)$							3445			
$4^1 8^1 11^1$ $(+8^1 11^3)$									3622	
$4^1 7^1 11^1$ $(+7^1 11^3)$										3667
$4^1 8^1 9^1$ $(+8^1 9^1 11^2)$									3972	
$4^1 7^1 9^1$ $(+7^1 9^1 11^2)$										4006
$4^1 8^1 11^1 13^1$ $(+8^1 11^3 13^1)$									4022	
$4^1 7^1 11^1 13^1$ $(+7^1 11^3 13^1)$										4056
$4^2 8^1$ $(+8^1 11^4)$									4433	
$4^2 7^1$ $(+7^1 11^4)$										4439

[a] The top row denotes the $S_1 \leftarrow S_0$ band excited prior to ionization, and the left-hand column shows the assignment given to each peak in the photoelectron spectrum.

S_1 vibrational modes with energies up to ~2000 cm^{-1} were prepared, four of which are relevant here; the origin, 6_0^1 ($\equiv 13_0^1$ in pFT), 5_0^1 ($\equiv 11_0^1$ in pFT) and 3_0^1 ($\equiv 7_0^1$ in pFT). Ionization was performed either with the same wavelength as that used for excitation (for modes with energies > 800 cm^{-1}), or with a shorter wavelength (for modes with energies < 800 cm^{-1}). In the one color experiments the available ion energies were about half of those for the equivalent pFT modes studied here owing to the higher ionization potential of pDFB, and therefore some of the ion modes analogous to the ones we observe were not energetically accessible. The second study describes ZEKE experiments performed by Müller-Dethlefs and co-workers.[14] In these experiments seven S_1 vibrational modes with energies up to ~1250 cm^{-1} were prepared, four of which are relevant here: the origin, 6_0^1, 3_0^1, and 27_0^1 ($\equiv 37_0^1$ in pFT). The ionization wavelength was scanned to obtain the ZEKE spectrum, giving ion energies up to ~3100 cm^{-1} above the ionization potential, and the spectra are much better resolved than those in ref 2.

The forms of the pFT photoelectron spectra shown here and the assignments given to them are in good agreement with the pDFB work. As for pDFB, all the strong peaks that appear are due to the excitation of ion vibrational modes that are totally symmetric except for the mode that has been prepared in S_1. A series of strong peaks appears in each of the photoelectron spectra shown in Figure 1, taking the form X^m, $X^m 13^1$, $X^m 11^1$, $X^m 9^1$, and $X^m 11^2$, where *m* quanta of mode X have been prepared in S_1; this series is indicated on each spectrum. In the photoelectron spectrum following the unresolved excitation of $37_0^1 + 16_0^2$, two such series can be identified because each band gives a characteristic photoelectron spectrum. The 10^1 spectrum also shows evidence of a series due to a second excited mode, but this has not been possible to assign. The presence of a strong X^m peak in each photoelectron spectrum is in agreement with the usual Franck−Condon propensity for this type of molecule,[1−4] and is also observed for pDFB with one exception (see later). The pDFB analogues of the modes ν_{11} and ν_{13} (both of which are ring bends) are active in all the relevant photoelectron spectra given in refs 2 and 14. In both molecules these two modes are also active in the $S_1 \leftarrow S_0$ excitation spectrum.[7,8,13] The pFT mode ν_9, a CH rock that appears in combinations with the excited mode in each photoelectron spectrum, also appears strongly in some of the relevant pDFB photoelectron spectra in refs 2 and 14. However, in a number of cases there was insufficient energy to form it. In neither molecule does this mode appear strongly in the excitation spectrum.[7,8,13]

A recurring feature of the photoelectron spectra in Figure 1 is the presence of surprisingly intense features at X^1 + ~1575 cm^{-1}. Inspection of the pDFB ZEKE spectrum following excitation of the S_1 origin[14] reveals an intense peak assigned as 2^1 only a few wavenumbers away from a smaller peak, assigned 5^2. Although ν_2 (a ring stretch) is therefore active in the pDFB photoelectron spectra, it is absent in the excitation spectrum. The analogy between pFT and pDFB (see Table 1) leads us to the conclusion that, for the pFT ion with our experimental resolution, 11^2 is coincident with 4^1. Consequently, relevant peaks have been assigned as a mixture of 4^1 and 11^2. Although the ratio of the two cannot be determined in this work, there is evidence that 4^1 is in fact the major component, see later. In complete analogy with pDFB, ν_4 is absent in the excitation spectrum.[7,8,13]

In summary, the main active modes in the excitation spectra of both pFT and pDFB are the ring breathing modes ν_{11} and ν_{13} (ν_5 and ν_6 in pDFB). On ionization these two modes remain active, but the CH rock ν_9 (ν_4 in pDFB) and the ring stretch ν_4 (ν_2 in pDFB) are also active. To understand this behavior, ab initio calculations with the complete active space self-consistent field (CASSCF) method with the 6-31G(d,p) basis set have been performed for the S_0, S_1, and ion ground states.[16] The active space was chosen to consist of the six π molecular orbitals of the benzene ring. No orbitals were frozen during the CASSCF procedure, and the geometry of each state was optimized to its minimum energy structure. The calculations were performed with the MOLCAS 5.2 program.[17] The relevant molecular orbitals for all three states are very similar and involve primarily the π system of the benzene ring. The resulting geometries of the three electronic states show that there are substantial changes in the C−C bond lengths. In particular, the benzene ring geometry in the ion ground state is very distorted with the C−C bonds nearest to F or CH_3 substantially longer than the other C−C bonds. The geometries adopted in both S_0 and S_1 give C−C bonds that are more comparable in length, although all are longer in S_1 than in S_0. This explains the activity of ν_4 in the photoelectron spectrum, its lack of activity in excitation, and the activity of ν_{11} and ν_{13} in both cases. These geometries also explain the activity of ν_9 in the photoelectron spectrum because the mode involves ring distortion as well as a CH rock. The calculations show in addition that the C−F bond length is similar in the S_0 and S_1 states, but substantially shorter in the

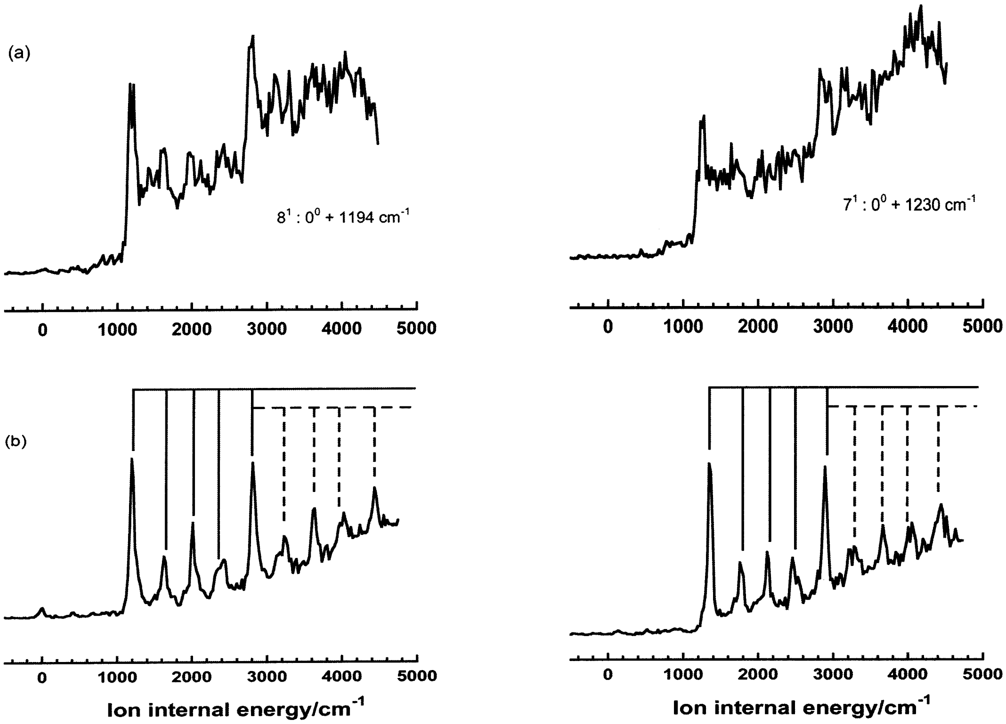

Figure 2. (a) Nanosecond and (b) picosecond photoelectron spectra following the excitation of the 8_0^1 and 7_0^1 bands as labeled. The characteristic series is labeled as in Figure 1, and a similar higher energy series also appears, taking the form X^m4^1, $X^m4^113^1$, $X^m4^111^1$, $X^m4^19^1$, and X^m4^2.

ion. This would suggest that ν_7, the C$-$F stretching mode, should be active in the photoelectron spectrum, but this is not observed. This fact remains unexplained.

One marked breakdown in the analogy between pDFB and pFT arises from the comparison between the 6_0^1 (pDFB) and 13_0^1 (pFT) photoelectron spectra, which should be equivalent. In the pDFB case the photoelectron spectrum[2] shows 6^2 to be the most intense of the peaks in the ν_6 progression; this shift in the Franck$-$Condon maximum to $\Delta v = 1$ is supported by the corresponding ZEKE spectrum .[14] Contrastingly, inspection of the relevant photoelectron spectrum in Figure 1 shows that for pFT the propensity for $\Delta v = 0$ prevails.

Small but reproducible peaks are present in the photoelectron spectra shown in Figure 1. Comparison with pDFB[2,14] suggests that these peaks are caused by single quantum excitation of the low-frequency asymmetric modes, ν_{16}, ν_{24}, and ν_{25}. Our photoelectron spectra following excitation of ν_{25} and ν_{38} enable us to tentatively assign some of the peaks to the excited mode in combination with either ν_{16} or ν_{25} (see Table 2). Arguments for the appearance of asymmetric modes in both excitation and ionization have been well rehearsed for pDFB.[13,14]

The photoelectron spectra obtained following the excitation of the 8_0^1 and 7_0^1 bands are shown in Figure 2. It will be seen that when excitation and ionization are performed with nanosecond laser pulses (upper panels) there is a definite loss of vibrational structure in the photoelectron spectra. This loss, which is almost complete in the case of the 7_0^1 spectrum, is attributed to intramolecular vibrational energy redistribution (IVR) which has been shown to have a lifetime of ~15 ps at this level of S_1 excitation.[5,6] Therefore, each of these photoelectron spectra can be thought of as a sum of the photoelectron spectra emanating from each of the levels to which energy redistribution has occurred. Despite the small difference in S_1 internal energy for the two modes (36 cm^{-1}) the loss of structure is significantly more pronounced for the higher energy mode. The modes in question are a C$-$CH$_3$ stretch (ν_8) and a C$-$F stretch (ν_7), and so if the torsional motion of the methyl group is the key to rapid IVR it seems unlikely that excitation of ν_7 would promote more efficient IVR than excitation of ν_8. Work is in progress to attempt to explain this observation and other aspects of the IVR behavior of pFT, both through modeling and through picosecond time-dependent studies[18] following on from ref 6.

In the lower panels of Figure 2 are shown the corresponding photoelectron spectra when excitation and ionization are performed with overlapped 1 ps laser pulses. In this case it can be seen that vibrational resolution is recovered. Vibrational assignments of the peaks in these two picosecond photoelectron spectra have been made, and the results are included in Tables 1 and 2. It will be seen that the characteristic series of peaks mentioned above appears for these two photoelectron spectra as well and that because of the higher energy available to the ion a further series is also present, taking the analogous form X^m4^1, $X^m4^113^1$, $X^m4^111^1$, $X^m4^19^1$, and X^m4^2. It is the presence of this higher series that leads us to suggest that the X^14^1 peak is likely to be more intense than the isoenergetic X^111^2 peak. The assignment of the lower energy part of the 7_0^1 photoelectron spectrum exactly reproduces the assignment of the equivalent (3_0^1) spectrum in pDFB. As ν_8 in pFT involves the methyl group, there is no analogous mode in pDFB. The assignments and deduced vibrational frequencies given here replace the preliminary ones given in ref 6. In our picosecond time-resolved studies of these two modes, we have found that the photoelectron spectra following a 100 ps delay are very similar to the nanosecond photoelectron spectra.

Conclusions

The frequencies of 12 vibrational modes of the *p*-fluorotoluene ion have been deduced by use of nanosecond and picosecond laser photoelectron spectroscopy in which 10 different vibrational modes were prepared in S_1 prior to ionization. For S_1 energies below ~900 cm^{-1}, the nanosecond photoelectron spectra show clearly resolved vibrational structure. For S_1

energies above ~1100 cm^{-1}, the photoelectron spectra show resolved vibrational structure only when picosecond pulses are used to excite and ionize. This is caused by intramolecular dynamics in S_1 occurring on a subnanosecond time scale.

Acknowledgment. We are indebted to Mike Towrie and Pavel Matousek of the Lasers for Science Facility at the Rutherford Appleton Laboratory for their assistance in obtaining the two picosecond photoelectron spectra shown in this paper. We also thank David M. Rogers and Jonathan D. Hirst for performing ab initio calculations of pFT geometries. P.T.W. thanks the EPSRC for a Doctoral Training Account studentship. This work was supported by EPSRC Grant GR/M83579.

References and Notes

(1) Sekreta, E.; Reilly, J. P. *Chem. Phys. Lett*. **1988**, *149*, 482.

(2) Sekreta, E.; Viswanathan, K. S.; Reilly, J. P. *J. Chem. Phys*. **1989**, *90*, 5349.

(3) Meek, J. T.; Long, S. R.; Reilly, J. P. *J. Phys. Chem*. **1982**, *86*, 2809.

(4) Anderson, S. L.; Goodman, L.; Kroghjespersen, K.; Ozkabak, A. G.; Zare, R. N.; Zheng, C. F. *J. Chem. Phys*. **1985**, *82*, 5329.

(5) Moss, D. B.; Parmenter, C. S. *J. Chem. Phys*. **1993**, *98*, 6897.

(6) Davies, J. A.; Reid, K. L.; Towrie, M.; Matousek, P. *J. Chem. Phys*. **2002**, *117*, 9099.

(7) (a) Dolson, D. A.; Stone, B. M.; Parmenter, C. S. *Chem. Phys. Lett*. **1981**, *81*, 360. (b) Parmenter, C. S.; Stone, B. M. *J. Chem. Phys*. **1986**, *84*, 4710. (c) Ju, Q.; Parmenter, C. S.; Stone, T. A.; Zhao, Z. Q. *Isr. J. Chem*. **1997**, *37*, 379.

(8) Okuyama, K.; Mikami, N.; Ito, M. *J. Phys. Chem.* **1985**, *89*, 5617.

(9) Takazawa, K.; Fujii, M.; Ito, M. *J. Chem. Phys.* **1993**, *99*, 3205.

(10) (a) Townsend, D. P.; Reid, K. L. *J. Chem. Phys*. **2000**, *112*, 9783. (b) Reid, K. L.; Field, T. A.; Towrie, M.; Matousek, P. *J. Chem. Phys*. **1999**, *111*, 1438.

(11) Jarzecki, A. A.; Davidson, E. R.; Ju, Q.; Parmenter, C. S. *Int. J. Quantum Chem*. **1999**, *72*, 249.

(12) (a) Mulliken, R. S. *J. Chem. Phys*. **1955**, *23*, 1997. (b) Hickman, C. G.; Gascooke, J. R.; Lawrance, W. D. *J. Chem. Phys*. **1996**, *104*, 4887.

(13) Knight, A. E. W.; Kable, S. H. *J. Chem. Phys.* **1988**, *89*, 7139.

(14) Reiser, G.; Rieger, D.; Wright, T. G.; Müller-Dethlefs, K.; Schlag, E. *J. Chem. Phys.* **1993**, *97*, 4335.

(15) See, for example: (a) Bondybey, V. E.; Miller, T. A.; English, J. H. *J. Chem. Phys.* **1979**, *71*, 1088. (b) Bondybey, V. A.; Miller, T. A. *J. Chem. Phys*. **1980**, *73*, 3053. (c) Bondybey, V. E. *J. Chem. Phys*. **1979**, *71*, 3586.

(16) Rogers, D. M.; Hirst, J. D. Private communication.

(17) MOLCAS version 5.2: Andersson, K.; Barysz, M.; Bernhardsson, A.; Blomberg, M. R. A.; Carissan, Y., Cooper, D. L.; Cossi, M.; Fleig, T.; Fülscher, M. P.; Gagliardi, L.; de Graaf, C.; Hess, B. A.; Karlström, G.; Lindh, R.; Malmqvist, P.-Å.; Neogrády, P.; Olsen, J.; Roos, B. O.; Schimmelpfennig, B.; Schütz, M.; Seijo, L.; Serrano-Andrés, L.; Siegbahn, P. E. M.; Stålring, J.; Thorsteinsson, T.; Veryazov, V.; Wierzbowska, M.; Widmark, P.-O. *MOLCAS* version 5.2; Lund University, Sweden, 2001.

(18) Davies, J. A.; Bellm, S. M.; Whiteside, P. T.; Reid, K. L.; Towrie, M.; Matousek, P. (unpublished work).